Available online at www.sciencedirect.com

ScienceDirect

Mendeleev Commun., 2023, **33**, 340–342

Mendeleev Communications

Internalization of PLGA nanoparticles coated with poloxamer 188 in glioma cells: a confocal laser scanning microscopy study

Dmitry V. Beigulenko,*[a] Aleksey S. Semyonkin,[a] Julia A. Malinovskaya,[a] Pavel A. Melnikov,[b] Ekaterina I. Medyankina,[c] Tatyana S. Kovshova,[a] Yulia V. Ermolenko[a] and Svetlana E. Gelperina[a]

[a] *D. I. Mendeleev University of Chemical Technology of Russia, 125047 Moscow, Russian Federation. E-mail: beigulenkodm@gmail.com*

[b] *V. P. Serbsky National Medical Research Centre of Psychiatry and Narcology, 119034 Moscow, Russian Federation*

[c] *N. I. Pirogov Russian National Research Medical University, 117997 Moscow, Russian Federation*

DOI: 10.1016/j.mencom.2023.04.014

Internalization of poloxamer 188-coated PLGA nanoparticles (NPs) in GL261 murine glioma cells was studied using confocal laser scanning microscopy. For visualization, both poloxamer 188 (P188) and PLGA were labeled covalently with fluorescent dyes Rhodamine B and Cyanine5, respectively. The results indicated that the PLGA NPs coated with poloxamer 188 enter a cell as an integral core–shell structure, which can be helpful for gaining further insight into the *in vivo* performance of surfactant-coated polymeric NPs as core–shell delivery systems.

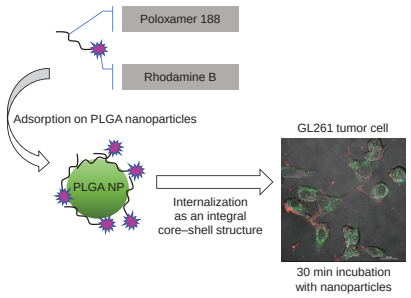

Keywords: poloxamer 188, confocal laser scanning microscopy (CLSM), polylactide-co-glycolide nanoparticles (PLGA NPs), GL261 murine glioma cells, Rhodamine B.

Nanoparticles (NPs) of biocompatible and biodegradable poly(lactic-co-glycolic acid) (PLGA) are promising drug nanocarriers because of the safety, versatility, and commercial availability of this polymer.[1] Many properties of PLGA-based nanocarriers, such as the rate of *in vivo* degradation and the profile of drug release, are tunable. However, the nanoparticles tend to accumulate in organs of the mononuclear phagocytic system (MPS), such as liver and spleen. This tendency is a serious limitation for drug delivery to non-MPS-related targets. An effective strategy to overcome this drawback is to modify the NP surface using surfactants, which improve biodistribution. Indeed, surface properties such as hydrophobicity determine the composition of a protein corona (a layer of plasma proteins adsorbed by nanoparticles from blood), which plays a crucial role in the recognition of NPs by the MPS and their circulation parameters and ability to traverse various blood–tissue barriers. Thus, the coating of drug-loaded PLGA NPs with poloxamer 188, a triblock copolymer of polyethylene oxide and polypropylene oxide (P188, PEO_{38}-PPO_{29}-PEO_{38}), enabled their trafficking across the blood–brain barrier (BBB) and brain delivery of encapsulated drugs, which was evidenced by pharmacological effects of these delivery systems in model CNS pathologies including intracranial glioma in rats.[2] It was hypothesized that a coating with P188 attracts certain apolipoproteins to the NP surface, and these apolipoproteins mediate the interaction of NPs with blood vessel endothelial cells followed by the NP transcytosis into the brain. Enhanced interaction of PLGA NPs with various cells due to the P188 coating was also observed in *in vitro* studies.[3,4]

As shown previously, the coating of solid NPs with poloxamers creates core–shell nanosystems where a hydrophilic shell is formed by PEO segments of a poloxamer; in a biological environment, this shell can be lost or displaced by other molecules, for example, blood plasma proteins.[5] Thus, an essential factor responsible for the efficacy of such delivery systems is the shell stability during its trafficking to the target cells. Although P188-coated PLGA NPs have demonstrated considerable efficacy, the biological fate of this core–shell delivery system remains to be elucidated. The aim of this study was to evaluate the stability of the P188-coated PLGA NPs in *in vitro* experiments and to gain insight into the interaction of these NPs with model GL261 murine glioma cells using confocal laser scanning microscopy (CLSM). For this purpose, both PLGA and P188 were labeled with Cyanine5 (Cy5) and Rhodamine B (RhB), respectively. Covalent bonding of these dyes to the polymer end groups ensured the retention of the labels in biological media for the reliable CLSM detection of both the NPs and the P188 coating.

The fluorescent poloxamer 188 derivative was synthesized by the conjugation of the polymer to the fluorescent dye Rhodamine B using carbodiimide chemistry; a Rhodamine B to P188 molar ratio was ~2 : 1 (Scheme 1).[6,7]

The reaction was carried out while stirring the mixture for three days at room temperature. The use of dimethylformamide (DMF) as a solvent was convenient because the P188 conjugate was poorly soluble in DMF at low temperature and precipitated upon cooling. The precipitated product was washed with a cold mixture of DMF and diethyl ether and then purified by preparative gel-filtration chromatography. The yield was 55%.

© 2023 Mendeleev Communications. Published by ELSEVIER B.V. on behalf of the N. D. Zelinsky Institute of Organic Chemistry of the Russian Academy of Sciences.

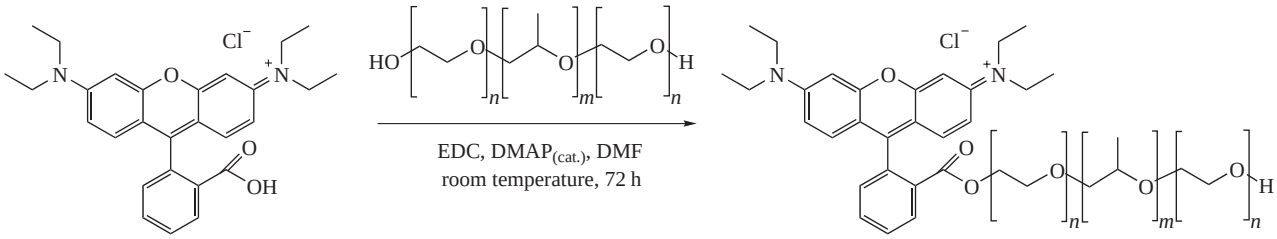

Scheme 1

Poloxamer 188 reacts with the dye *via* its terminal hydroxyl groups to yield two types of labeled block-copolymer molecules, *i.e.*, mono- and disubstituted conjugates. However, according to the MALDI mass spectrometry data (Online Supplementary Materials, Figure S1), the average molecular weight of the product increased by only ~400 Da (from 8.4 to 8.8 kDa), whereas the molecular weight of Rhodamine B is 479 Da. Therefore, it is most likely that the product was a mixture of a monosubstituted P188 derivative and an unsubstituted polymer. At the same time, the IR spectra of the product (Figures S2–S3) exhibited a characteristic absorption band due to C=O bonds at 1721 cm^{-1} , which confirmed the binding of the dye to P188, whereas the bands at 2900 and 1100 cm^{-1} indicated the preservation of the polymer chain. The ^1H NMR spectrum (Figure S4) seems uninformative: only peaks corresponding to CH bonds in the alkyl groups of the polymer are visible in a strong field and aromatic groups near 7.5 ppm.

To assess the effect of the substitution of hydroxyl groups in P188 on its surfactant properties, we compared critical micelle concentrations (CMCs) of the P188–RhB conjugate and the parent poloxamer 188. The CMC values were obtained from the dependence of the derived count rate (DCR) on the decimal logarithm of the surfactant concentration in water in the absence of attenuation as described previously[8] (Figure S5). The conjugation of P188 with Rhodamine B led to a decrease in the CMC (CMCs of 1.0 and 3.1 mg ml^{-1}, respectively),[†] which was most probably due to an alteration of the surfactant chemical structure. The CMC of unmodified P188 found in this study is consistent with published data.[8]

The PLGA NPs used for the evaluation of P188 adsorption were prepared by a high pressure o/w emulsification–solvent evaporation technique as described previously.[9–12] These NPs had an average diameter of 110 ± 2 nm and a narrow size distribution (PDI = 0.16 ± 0.01; dynamic light scattering, DLS); their zeta potential was −23.5 ± 1.1 mV. To study the adsorption, the PLGA NPs were resuspended in an aqueous solution of P188–RhB with a concentration of 1% (w/v); aliquot portions of the suspension were centrifuged to separate the NPs. Then, the precipitates were dissolved in DMSO, and the amount of adsorbed P188–RhB was determined by spectrophotometry at 555 nm.[‡] Adsorption of unmodified P188 was determined by measuring the absorbance of its complex with iodine as described previously.[13] The conjugation of P188 to Rhodamine B did not affect its adsorption capacity; on the contrary, the amount of P188–RhB found in the NP precipitate after 1 h of incubation was even higher than that of unmodified P188: 0.38 ± 0.04 and 0.14 ± 0.09 mg m^{-2}, respectively. This observation correlates with the results obtained by Adler and Parmryd,[14] who also found that labeling poloxamers with a fluorescent dye did not interfere with their adsorption onto the NP polymeric surface. Stability of the P188–RhB conjugate was evaluated in model media commonly used in biological experiments, including phosphate buffered saline (PBS, pH 7.4), Dulbecco's modified eagle's medium (DMEM) for cell cultures, and human blood plasma. After a 2-h incubation of the conjugate in these media at 37 °C, a fluorescent impurity was isolated using thin layer chromatography (TLC) (Figure S6), and its content was determined by spectrofluorimetry.[§] Table 1 shows that the resulting P188-RhB conjugate initially had a low free dye content. After the incubation, the fluorescent impurity content of the incubation media increased slightly, possibly due to partial hydrolysis of ester bonds in the conjugate; however, it did not exceed 0.3% (Figure S1). The conjugate can be reliably detected by fluorescent microscopy.

Importantly, conjugation of Rhodamine B with P188 did not influence considerably the optical parameters of this dye (Figures S7, S8). Thus, the absorption maxima of Rhodamine B and P188–RhB at 554 and 561 nm, respectively, were close. Similarly, the shifts of the fluorescence maxima at an excitation wavelength of 488 nm were minor: 491 and 577 nm for Rhodamine B and 492 and 585 nm for P188–RhB, respectively.

The conjugation with P188 did not affect the quantum yield and brightness of Rhodamine B; these parameters are essential for dye visualization through fluorescence microscopy (Table 1). The dye and the conjugate demonstrated nearly identical quantum yields and comparable brightness values on a unit weight basis.

Table 1 Quantum yield and brightness of Rhodamine B and P188–RhB conjugate in PBS (n = 3, P = 0.95).

Compound	Quantum yield	Brightness/l g^{-1} cm^{-1}
Rhodamine B	0.27	4.3×10^{-4}
P188–RhB	0.27	5.3×10^{-4}

As mentioned above, in order to enable *in vitro* visualization, the core PLGA NPs were prepared using a polymer with the covalently bonded fluorescent dye Cyanine5 (PLGA–Cy5)[3,8] and then coated with P188–RhB. For coating, the PLGA–Cy5 NPs were resuspended in a solution of P188–RhB and the suspension was incubated for 30 min. The coated NPs were introduced into the GL261 murine glioma cell culture and incubated with the cells for 15, 30, and 45 min. Since the NPs generally tend to accumulate in cell lysosomes, these organelles were labeled with a lysotracker (LysoTracker Green DND-26, LT). A Nikon A1R inverted confocal microscope (Nikon, USA) was used to visualize the distribution of the double-labeled nanocarrier in cells. The images were processed using the NIS-Elements AR software (Nikon, USA). The images were obtained in three fluorescence channels corresponding to the fluorescence maxima of LT (Alexa channel), RhB (DiI channel) and Cy5 (Cy5 channel), respectively, which were then combined into a merged image (Merged channel) and in the differential interference contrast (DIC channel) (Figure 1).

[†] The CMCs and PLGA NP characteristics were measured using a ZetaSizer Nano ZS instrument (Malvern Instruments Ltd, UK).

[‡] Absorbance spectra were measured using a UV-1900i spectrophotometer (Shimadzu, Japan).

[§] Fluorescence spectra were measured using an RF-6000 spectrofluorometer (Shimadzu, Japan).

Table 2 Pearson and Manders colocalization coefficients for Rhodamine B and Cyanine5 in GL261 cells.

Time/ min	Colocalization coefficients					
	Pearson coefficient			Manders coefficient		
	LT/ PLGA–Cy5	LT/P188–RhB	PLGA–Cy5/ P188–RhB	LT/ PLGA-Cy5	LT/P188–RhB	PLGA–Cy5/ P188–RhB
15	0.15 ± 0.11	0.17 ± 0.06	0.25 ± 0.11	0.30 ± 0.06	0.22 ± 0.05	0.48 ± 0.15
30	0.28 ± 0.03	0.25 ± 0.06	0.38 ± 0.11	0.36 ± 0.04	0.29 ± 0.05	0.57 ± 0.26
45	0.30 ± 0.07	0.26 ± 0.15	0.47 ± 0.08	0.36 ± 0.04	0.31 ± 0.14	0.61 ± 0.22

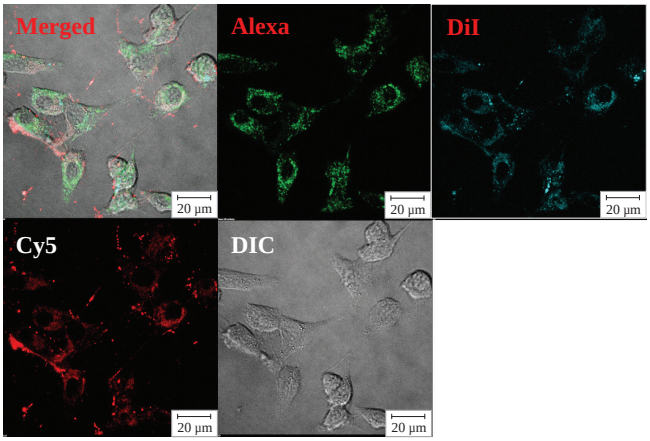

Figure 1 Visualization of the biodistribution of PLGA–Cy5 NPs coated with P188–RhB after 30 min of incubation with GL261 cell culture.

The colocalization of P188–RhB and PLGA–Cy5 NPs in model cells was estimated according to the confocal microscope data using the Pearson and Manders colocalization coefficients. The degree of colocalization between Rhodamine B and Cyanine5 in the cells was quantified for the P188–RhB/LT, P188–RhB/PLGA–Cy5, and PLGA–Cy5/LT pairs (Table 2). The colocalization of two fluorescent labels was considered reliable if the colocalization coefficients were above 0.5.[15]

Lower Pearson and Manders coefficients obtained for the first 15 min of incubation (0.25 and 0.48, respectively) indicate that, at early time points, a portion of the free poloxamer was more rapidly taken up by the cells as compared to the PLGA NPs. Further incubation of the NPs with the cells (for 30–45 min) led to an increase in the average colocalization coefficients (from 0.38 and 0.57 to 0.47 and 0.61 for the Pearson and Manders coefficients, respectively), which indicates a high level of overlapping of the signals of PLGA–Cy5 and P188–RhB. Therefore, according to Manders colocalization coefficients of 0.57–0.61, the P188–RhB coating was still retained on the surface of the internalized PLGA NPs after 45-min incubation with the cells (Table 3). Using these data, we can conclude that a large percentage of PLGA NPs entering the cells retained the poloxamer on their surface.

Interestingly, despite the known tendency of NPs to accumulate in lysosomes,[15] the colocalization coefficients between the PLGA–Cy5/lysosome and P188–RhB/lysosome pairs were 0.2–0.35 throughout the experiment, respectively, suggesting that only a small percentage of PLGA NPs and P188–RhB accumulated in lysosomes. This finding is also in contrast to our previous results obtained in the U87 human glioma cells, where the PLGA–Cy5 NPs coated with P188 were colocalized with lysosomes. This phenomenon, most probably related to the specific features of GL261 cells, deserves further investigation.

In conclusion, the results of this study indicated that the PLGA NPs coated with poloxamer 188 enter a cell as an integral core–shell structure. These results are helpful for gaining further insight into the *in vivo* performance of surfactant-coated polymeric NPs as core–shell delivery systems.

The research was carried out within the state assignment of Ministry of Science and Higher Education of the Russian Federation (project FSSM-2022-0003). The authors are grateful to the D. I. Mendeleev Center for Collective Use of Scientific Equipment for performing the analytical tests.

Online Supplementary Materials

Supplementary data associated with this article can be found in the online version at doi: 10.1016/j.mencom.2023.04.014.

References

1 E. S. Trofimchuk, M. A. Moskvina, O. A. Ivanova, V. V. Potseleev, V. A. Demina, N. I. Nikonorova, A. V. Bakirov, N. G. Sedush and S. N. Chvalun, *Mendeleev Commun.*, 2020, **30**, 171.
2 S. Gelperina, O. Maksimenko, A. Khalansky, L. Vanchugova, E. Shipulo, K. Abbasova, R. Berdiev, S. Wohlfart, N. Chepurnova and J. Kreuter, *Eur. J. Pharm. Biopharm.*, 2010, **74**, 157.
3 Y. Malinovskaya, P. Melnikov, V. Baklaushev, A. Gabashvili, N. Osipova, S. Mantrov, Y. Ermolenko, O. Maksimenko, M. Gorshkova, V. Balabanyan, J. Kreuter and S. Gelperina, *Int. J. Pharm.*, 2017, **524**, 77.
4 E. L. J. Moya, S. M. Lombardo, E. Vandenhaute, M. Schneider, C. Mysiorek, A. E. Türeli, T. Kanda, F. Shimizu, Y. Sano, N. Maubon, F. Gosselet, N. Günday-Türeli and M.-P. Dehouck, *Int. J. Pharm.*, 2022, **621**, 121780.
5 J. C. Neal, S. Stolnik, E. Schacht, E. R. Kenawy, M. C. Garnett, S. S. Davis and L. Illum, *J. Pharm. Sci.*, 1998, **87**, 1242.
6 D. S. Pellosi, L. B. Paula, M. T. de Melo and A. C. Tedesco, *Mol. Pharm.*, 2019, **16**, 1009.
7 A. Russo, D. S. Pellosi, V. Pagliara, M. R. Milone, B. Pucci, W. Caetano, N. Hioka, A. Budillon, F. Ungaro, G. Russo and F. Quaglia, *Int. J. Pharm.*, 2016, **511**, 127.
8 V. Zhukova, N. Osipova, A. Semyonkin, J. Malinovskaya, P. Melnikov, M. Valikhov, Y. Porozov, Y. Solovev, P. Kuliaev, E. Zhang, B. A. Sabel, V. Chekhonin, M. Abakumov, A. Majouga, J. Kreuter, P. Henrich-Noack, S. Gelperina and O. Maksimenko, *Pharmaceutics*, 2021, **13**, 1145.
9 C. Chunhachaichana and T. Srichana, *J. Dispersion Sci. Technol.*, 2018, **40**, 1461.
10 M. W. Heron and B. C. Paton, *Anal. Biochem.*, 1968, **24**, 491.
11 E. Pereverzeva, I. Treschalin, M. Treschalin, D. Arantseva, Y. Ermolenko, N. Kumskova, O. Maksimenko, V. Balabanyan, J. Kreuter and S. Gelperina, *Int. J. Pharm.*, 2019, **554**, 161.
12 M. A. Merkulova, N. S. Osipova, O. O. Maksimenko, M. G. Gordienko and S. E. Gelperina, *Mendeleev Commun.*, 2021, **31**, 899.
13 F. Ahmed, P. Alexandridis and S. Neelamegham, *Langmuir*, 2001, **17**, 537.
14 J. Adler and I. Parmryd, *Methods Mol. Biol.*, 2013, **931**, 97.
15 G. C. Baltazar, S. Guha, W. Lu, J. Lim, K. Boesze-Battaglia, A. M. Laties, P. Tyagi, U. B. Kompella and C. H. Mitchell, *PloS ONE*, 2012, **7**, e49635.

Received: 12th October 2022; Com. 22/7023